

Direct Informed Sampling on Riemannian Manifolds via Loewner Order Lower Bounds

Phone Thiha Kyaw and Jonathan Kelly

Abstract—Informed sampling techniques accelerate sampling-based motion planners by focusing the search on promising regions of the state space, yet most existing methods rely on Euclidean heuristics that become inadmissible under configuration-dependent Riemannian metrics. While scalar eigenvalue bounds restore admissibility by uniformly scaling the Euclidean distance, they discard the directional structure of the metric, producing overly conservative informed sets. We propose a matrix-valued admissible heuristic that exploits the Loewner order on symmetric positive definite matrices to compute the tightest constant lower bound on the metric tensor while preserving its full directional structure. The Cholesky factorization of this bound defines a linear map to an isotropic Euclidean space in which the Riemannian informed set reduces to a standard prolate hyperspheroid, enabling direct, rejection-free sampling using existing algorithms. Experiments on manipulation tasks with a 6-DoF UR5, 7-DoF Franka, and 14-DoF PR2 under three distinct Riemannian metrics show that our heuristic produces consistently tighter informed sets than both the Euclidean and scalar eigenvalue bounds, accelerating convergence across multiple state-of-the-art asymptotically optimal planners.

Index Terms—Motion and Path Planning, Informed Sampling, Riemannian Geometry, Loewner Order

I. INTRODUCTION

Asymptotically optimal sampling-based planners, such as Rapidly-exploring Random Trees (RRT*) and Batch Informed Trees (BIT*), incrementally explore the configuration space using random sampling and asymptotically converge to the global optimum as the number of samples grows [1], [2], [3]. A key insight of direct informed sampling approaches is that convergence can be dramatically accelerated by focusing sampling on the *informed set*, the subset of the configuration space that could potentially include promising samples capable of improving the current best solution [4]. Under Euclidean metric costs, this set is a prolate hyperspheroid centered on the start–goal axis, and uniform samples can be drawn directly via an affine transformation of an n -dimensional unit ball.

Many robotics applications, however, require planning with respect to *configuration-dependent* cost structures that go beyond Euclidean distance. For instance, kinetic energy metrics weight the cost of motion by the manipulator’s mass matrix, producing shorter paths through low-inertia configurations [5], [6], [7], [8]. Other position-dependent metrics include manipulability [9], joint stiffness [10], and distance to kinematic singularities [11]. In all such cases, the cost of traversing a path depends on *where* the robot is in

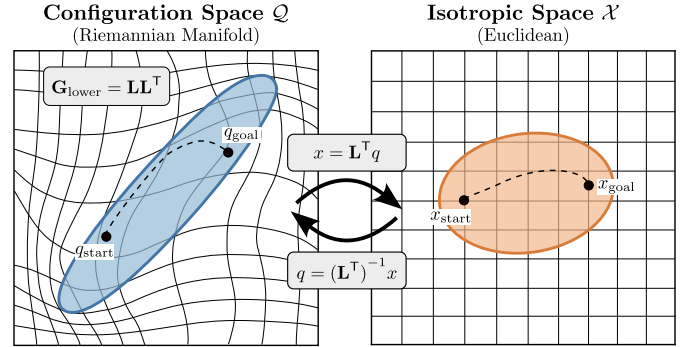


Fig. 1: Illustration of the proposed direct informed sampling approach for a Riemannian configuration space. The Cholesky factorization of a Loewner lower bound $G_{\text{lower}} = LL^T$ of the configuration-dependent metric tensor defines a linear isometry $x = L^T q$ that maps the anisotropic Riemannian informed set (blue) in the original configuration space to a prolate hyperspheroid (orange) in an isotropic Euclidean space. Direct sampling from the prolate hyperspheroid in the isotropic space produces rejection-free samples on the Riemannian informed set without requiring knowledge of the full metric field.

configuration space, captured mathematically by a Riemannian metric tensor that varies smoothly with the configuration.

Existing informed sampling methods cannot be applied directly to these Riemannian cost structures because they rely on an admissible heuristic—a lower bound on the true cost-to-go—that is unavailable under non-Euclidean metrics. Without one, planners must either sample uniformly over the entire configuration space, forgoing the convergence benefits of informed sampling, or default to the Euclidean distance as the heuristic. The latter option is not merely conservative; it is inadmissible under many non-Euclidean metrics. Under the kinetic energy metric, for example, the Euclidean heuristic overestimates the true geodesic distance for 99% of configuration pairs on high-DoF manipulators (as we show in Section VI-A), producing informed sets that fail to contain the true promising region. Even when a valid scalar heuristic can be constructed, for example, by scaling the Euclidean distance by the minimum eigenvalue of the metric tensor [12], the resulting informed set is still a prolate hyperspheroid and thus ignores the directional structure of the metric, assigning equal sampling density to all directions regardless of their associated eigenvalues.

In this paper, we address these limitations by introducing a direct informed sampling method based on the Loewner order on symmetric positive definite (SPD) matrices. Our key idea is to compute a constant SPD matrix that lower-bounds the configuration-dependent metric tensor everywhere in the space, preserving directional information that scalar bounds discard. The Cholesky factorization of this lower bound matrix defines an *isotropic* Euclidean space in which the

All authors are with the Space and Terrestrial Autonomous Robotic Systems (STARS) Laboratory, University of Toronto Institute for Aerospace Studies (UTIAS), Toronto, Ontario M3H 5T6, Canada (e-mail: {phone.thiha, jonathan.kelly}@robotics.utias.utoronto.ca).

Riemannian informed set reduces to a standard ellipsoid, enabling rejection-free direct sampling via well-known Euclidean techniques (Figure 1). To the best of our knowledge, this is the first method for direct informed sampling under configuration-dependent Riemannian metrics.

Our main contributions are as follows.

- We introduce a matrix-valued admissible heuristic via the Loewner order on SPD matrices that is provably at least as tight as the scalar (minimum eigenvalue) bound.
- We provide an efficient incremental algorithm for computing a maximal constant lower bound on the metric tensor from a sequence of pointwise evaluations.
- We show that the Loewner lower bound induces an isotropic space in which the Riemannian informed set is a standard prolate hyperspheroid, enabling direct informed sampling using existing Euclidean techniques.

II. RELATED WORK

Informed sampling has driven much of the recent progress in optimal planning, but existing heuristics for non-Euclidean cost structures are either restricted to kinodynamic settings or do not scale to high-dimensional configuration spaces (see Sections II-A and II-B). We construct a matrix-valued admissible heuristic from the Loewner order; Section II-C reviews its prior uses in robotics.

A. Informed Sampling for Optimal Planning

Direct informed sampling accelerates convergence of asymptotically optimal planners by restricting sampling to the *informed set*, the region of configuration space that could contain paths shorter than the current best solution [4]. Under Euclidean path length, this set is a prolate hyperspheroid, from which uniform samples can be drawn directly without rejection. Batch Informed Trees (BIT*) generalizes informed sampling to batches of random samples, processing them in order of admissible lower-bound estimates of potential solution cost [3]. Adaptively Informed Trees (AIT*) and Effort Informed Trees (EIT*) further relax the need for closed-form admissible heuristics by computing problem-specific cost-to-go estimates through a reverse search from the goal [13]. Greedy-RRT* (G-RRT*) instead accelerates convergence by biasing samples toward the current best path through a greedy variant of the informed set [14]. Despite these advances, the direct sampling step in all of these methods fundamentally relies on the Euclidean geometry of the informed set.

When the cost function is non-Euclidean, the informed set loses its ellipsoidal structure and direct sampling is no longer straightforward [15]. Prior efforts to address this have focused solely on kinodynamic planning. Yi et al. recast informed set sampling as a sub-level set problem, applying MCMC to draw samples from non-ellipsoidal regions [16]. Kunz et al. propose *Hierarchical Rejection Sampling*, which constructs a hierarchy of axis-aligned bounding boxes to improve acceptance rates over naive rejection sampling [17]. While both methods handle general informed set geometries, they rely on iterative or rejection-based procedures and do not recover the direct sampling achievable under the Euclidean metric; extending

direct informed sampling to non-Euclidean cost structures remains an open problem [18]. Our work addresses this in the geometric planning setting, where the non-Euclidean cost arises from a configuration-dependent Riemannian metric tensor rather than from differential constraints.

B. Admissible Heuristics on Non-Euclidean Spaces

Admissible heuristics for non-Euclidean costs have been studied primarily in kinodynamic settings. One approach uses sum-of-squares programming to derive admissibility certificates from system dynamics [19]. More recent work extends heuristic-guided search to kinodynamic planning without requiring a closed-form steering function [20]. Other approaches construct admissible bounds from precomputed motion primitive databases [21] or through dimensionality relaxation [22]. All of these methods, however, are tailored to kinodynamic settings and do not address planning under general configuration-dependent Riemannian metrics.

A complementary line of work constructs heuristics by approximating geodesic distances rather than computing them exactly [23]. On surfaces and graphs, landmark-based methods precompute distances to selected reference points and exploit the triangle inequality to construct admissible lower bounds [24], [25]. Scaling these methods to general high-dimensional Riemannian manifolds, however, requires solving the Eikonal equation [12], [26], which becomes computationally intractable as dimension grows. Several recent works address planning in non-Euclidean configuration spaces without fully resolving the heuristic problem. One line extends Graphs of Convex Sets to Riemannian manifolds via convex relaxation [27], and another establishes asymptotic optimality of RRT* and PRM* under general non-Euclidean metrics [28], but neither provides explicit heuristics for informed sampling. Recently, Kyaw and Kelly proposed a geometry-aware planning framework using a midpoint-based geodesic approximation that is accurate but not provably admissible, explicitly identifying heuristic design as important future work [8].

C. Loewner Order in Robotics

The Loewner order on symmetric matrices is foundational in robust control, where linear matrix inequalities encode stability and robustness constraints [29]. The closest analogues appear in belief-space planning, where scalar bounds on the maximum eigenvalue of the covariance matrix make sampling-based search tractable [30], [31], but these bounds collapse a configuration-dependent matrix to a scalar, discarding all directional information. Contraction-based approaches retain more structure; Singh et al. optimize a matrix-valued contraction metric via sum-of-squares programming and use a constant Loewner lower bound to define ellipsoidal robustness tubes around tracked trajectories [32]. In trajectory optimization, STOMP and CHOMP precompute a fixed precision matrix from finite-difference operators to define a Riemannian metric on the trajectory space [33], [34]; however, this matrix encodes temporal smoothness rather than configuration-space geometry. More broadly, semidefinite programming, which optimizes over the cone ordered precisely by the Loewner order, has been applied to related robotic problems such as collision-free region

construction [35] and state estimation [36]. In contrast, we exploit the Loewner order to construct a *matrix-valued* admissible heuristic that preserves the full directional structure of the metric tensor while enabling direct ellipsoidal informed sampling.

III. PRELIMINARIES

This section reviews the key concepts and establishes the notation used throughout the paper.

A. Riemannian Configuration Spaces

Let $\mathcal{Q} \subseteq \mathbb{R}^n$ denote the configuration space manifold, with each $q \in \mathcal{Q}$ representing a configuration of the robot. A Riemannian metric on \mathcal{Q} is a smoothly varying positive definite matrix $\mathbf{G}(q) \in \mathbb{S}_{++}^n$ that defines an inner product at each configuration [37]. The metric induces a notion of path length: for a piecewise smooth curve $\pi : [0, 1] \rightarrow \mathcal{Q}$, the Riemannian arc length is

$$L(\pi) = \int_0^1 \sqrt{\dot{\pi}(t)^\top \mathbf{G}(\pi(t)) \dot{\pi}(t)} dt. \quad (1)$$

The Riemannian distance between two configurations is defined as the infimum of arc lengths over all connecting curves,

$$d(q_x, q_y) = \inf_{\pi} L(\pi), \quad \pi(0) = q_x, \pi(1) = q_y. \quad (2)$$

When $\mathbf{G}(q) = \mathbf{I}$ for all q , the Riemannian distance reduces to the standard Euclidean distance $\|q_x - q_y\|_2$.

B. Informed Sampling for Optimal Planning

Given a start configuration q_{start} and a goal configuration q_{goal} , the optimal motion planning problem seeks a collision-free path π^* that minimizes the Riemannian arc length in (1) from q_{start} to q_{goal} . Asymptotically optimal sampling-based planners, such as RRT* [2], incrementally build a search tree over \mathcal{Q} and converge to π^* as the number of samples grows. This convergence can often be accelerated by using a distance estimate \hat{d} that lower-bounds the true distance (*admissible heuristic*), i.e., $\hat{d}(q_x, q_y) \leq d(q_x, q_y)$ for all $q_x, q_y \in \mathcal{Q}$, enabling the planner to prune configurations that provably cannot improve the current best solution. Many informed planners rely on such heuristics to focus sampling in promising regions of the configuration space [3], [13], [14].

Specifically, let c_{best} denote the cost of the current best solution. The *informed set* is the subset of configurations that could lie on a shorter path [4],

$$X_{\hat{f}} = \left\{ q \in \mathcal{Q} : \hat{d}(q_{\text{start}}, q) + \hat{d}(q, q_{\text{goal}}) < c_{\text{best}} \right\}. \quad (3)$$

Under the Euclidean metric ($\mathbf{G} = \mathbf{I}$), the natural heuristic is $\hat{d}(q_x, q_y) = \|q_x - q_y\|_2$, and $X_{\hat{f}}$ reduces to a prolate hyperspheroid with foci q_{start} and q_{goal} , from which uniform samples can be drawn directly via an affine transformation of the unit ball. However, when the cost is defined by a configuration-dependent Riemannian metric, the Euclidean distance is not necessarily admissible, and the geometry of $X_{\hat{f}}$ under a valid heuristic is no longer a standard hyperspheroid.

C. Loewner Order on Symmetric Matrices

The *Loewner order* is the partial order on symmetric matrices induced by the cone of positive semidefinite (PSD) matrices [38].

Definition 1 (Loewner order). *For symmetric matrices $\mathbf{A}, \mathbf{B} \in \mathbb{S}^n$, we write $\mathbf{A} \preceq \mathbf{B}$ if $\mathbf{B} - \mathbf{A}$ is positive semidefinite, i.e., $v^\top \mathbf{A} v \leq v^\top \mathbf{B} v$ for all $v \in \mathbb{R}^n$.*

The Loewner order is a partial order; that is, not all symmetric positive definite (SPD) matrices are comparable. In fact, a unique *greatest lower bound* (meet) generally does not exist for symmetric matrices unless the matrices are comparable in the Loewner order [39]. However, any finite collection $\{\mathbf{A}_1, \dots, \mathbf{A}_k\} \subset \mathbb{S}_{++}^n$ admits a *maximal lower bound* in the Loewner order, denoted $\bigwedge_{i=1}^k \mathbf{A}_i$, which is an SPD matrix dominated by every \mathbf{A}_i such that no strictly greater lower bound exists¹. This meet is not available in closed form but can be computed iteratively via pairwise meets, as we describe in Section IV².

IV. ADMISSIBLE HEURISTICS VIA LOEWNER BOUNDS

We first introduce a lower bound that exploits the Loewner order on SPD matrices to produce tighter estimates than scalar eigenvalue bounds. We then describe an iterative algorithm to compute this bound from a sequence of metric evaluations.

A. Matrix Lower Bound Heuristic

We begin by formalizing the notion of a constant matrix that lower-bounds the configuration-dependent metric tensor everywhere on the manifold.

Definition 2 (Loewner lower bound). *A constant symmetric positive definite matrix $\mathbf{G}_{\text{lower}} \in \mathbb{S}_{++}^n$ is a Loewner lower bound for the metric tensor \mathbf{G} if it satisfies the Loewner order (Definition 1) everywhere on \mathcal{Q} , i.e., $\mathbf{G}_{\text{lower}} \preceq \mathbf{G}(q), \forall q \in \mathcal{Q}$.*

A natural approach to satisfy this definition is to scale the Euclidean distance by the global minimum eigenvalue of $\mathbf{G}(q)$, which yields the simplest lower bound estimate for Riemannian geodesic distance [12], [32].

Definition 3 (Scalar distance lower bound). *Let $\lambda_{\min} = \inf_{q \in \mathcal{Q}} \lambda_{\min}(\mathbf{G}(q))$ denote the global minimum eigenvalue of the metric tensor, and define the isotropic lower-bound matrix $\mathbf{G}_\lambda = \lambda_{\min} \mathbf{I}$. The scalar distance lower bound is*

$$\hat{d}_\lambda(q_x, q_y) = \sqrt{\lambda_{\min}} \|q_x - q_y\|_2 = \|q_x - q_y\|_{\mathbf{G}_\lambda}. \quad (4)$$

While the scalar bound ensures admissibility by scaling distances uniformly, it can be overly conservative. We propose a more general distance estimate that replaces the configuration-dependent Riemannian metric with a tighter constant matrix.

Definition 4 (Matrix distance lower bound). *Let $\mathbf{G}_{\text{lower}} \in \mathbb{S}_{++}^n$ be a Loewner lower bound for \mathbf{G} (Definition 2), and let*

¹The order is defined on all symmetric matrices; here we restrict to Riemannian metric evaluations, which are symmetric positive definite.

²With a slight abuse of terminology, we use the word “meet” to refer to this specific constructed maximal lower bound.

$\mathbf{G}_{\text{lower}} = \mathbf{L}\mathbf{L}^\top$ denote its Cholesky factorization. The matrix distance lower bound is the function $\hat{d}: \mathcal{Q} \times \mathcal{Q} \rightarrow \mathbb{R}_{\geq 0}$,

$$\hat{d}(q_x, q_y) = \|q_x - q_y\|_{\mathbf{G}_{\text{lower}}} = \left\| \mathbf{L}^\top (q_x - q_y) \right\|_2. \quad (5)$$

Note that the scalar bound in (4) is a special case of the matrix bound, corresponding to the (isotropic) Loewner lower bound $\mathbf{G}_{\text{lower}} = \mathbf{G}_\lambda = \lambda_{\min} \mathbf{I}$. Because \mathbf{G}_λ is the largest isotropic matrix dominated by $\mathbf{G}_{\text{lower}}$, the matrix bound is always at least as tight as the scalar bound, and strictly tighter in directions where $\mathbf{G}_{\text{lower}}$ has eigenvalues greater than λ_{\min} .

Theorem 1 (Tightness relative to scalar bound). *The matrix distance lower bound \hat{d} dominates the scalar bound \hat{d}_λ*

$$\hat{d}_\lambda(q_x, q_y) \leq \hat{d}(q_x, q_y), \quad \forall q_x, q_y \in \mathcal{Q},$$

with equality if and only if $q_x - q_y$ is an eigenvector of $\mathbf{G}_{\text{lower}}$ corresponding to eigenvalue λ_{\min} .

Proof. Let $v = q_x - q_y$. Since $\lambda_{\min} \mathbf{I} \preceq \mathbf{G}_{\text{lower}}$,

$$v^\top \mathbf{G}_{\text{lower}} v \geq v^\top (\lambda_{\min} \mathbf{I}) v = \lambda_{\min} \|v\|_2^2.$$

Taking square roots gives $\hat{d}(q_x, q_y) \geq \hat{d}_\lambda(q_x, q_y)$. Equality holds if and only if $\mathbf{G}_{\text{lower}} v = \lambda_{\min} v$, i.e., v is an eigenvector of $\mathbf{G}_{\text{lower}}$ corresponding to λ_{\min} . \square

As the following theorem shows, the Loewner bound on the metric tensor is sufficient to guarantee that \hat{d} in (5) never overestimates the true geodesic distance.

Theorem 2 (Admissibility of matrix distance lower bound). *If $\mathbf{G}_{\text{lower}} \preceq \mathbf{G}(q)$ for all $q \in \mathcal{Q}$, then the matrix distance lower bound \hat{d} is admissible for the true geodesic distance d ,*

$$\hat{d}(q_x, q_y) \leq d(q_x, q_y), \quad \forall q_x, q_y \in \mathcal{Q}.$$

Proof. Let $\pi: [0, 1] \rightarrow \mathcal{Q}$ be any piecewise smooth curve from q_x to q_y . Since $\mathbf{G}_{\text{lower}} \preceq \mathbf{G}(q)$ for all $q \in \mathcal{Q}$,

$$\begin{aligned} L(\pi) &= \int_0^1 \sqrt{\dot{\pi}^\top \mathbf{G}(\pi) \dot{\pi}} dt \geq \int_0^1 \left\| \mathbf{L}^\top \dot{\pi} \right\|_2 dt \\ &\geq \left\| \mathbf{L}^\top (q_y - q_x) \right\|_2 = \hat{d}(q_x, q_y). \end{aligned}$$

The infimum over all curves yields $\hat{d}(q_x, q_y) \leq d(q_x, q_y)$. \square

An immediate consequence is that the matrix lower bound generalizes the standard Euclidean distance heuristic.

Corollary 1 (Euclidean special case). *When $\mathbf{G}_{\text{lower}} = \mathbf{I}$, the matrix distance lower bound reduces to the standard Euclidean distance, $\hat{d}(q_x, q_y) = \sqrt{(q_x - q_y)^\top \mathbf{I} (q_x - q_y)} = \|q_x - q_y\|_2$.*

While Corollary 1 recovers the Euclidean case, the converse does not hold; that is, using the Euclidean distance as a heuristic for any Riemannian metric can easily violate admissibility.

Remark 1. *Corollary 1 shows that the Euclidean distance corresponds to $\mathbf{G}_{\text{lower}} = \mathbf{I}$, which by Theorem 2 is admissible only if $\mathbf{I} \preceq \mathbf{G}(q)$ for all q , i.e., $\lambda_{\min}(\mathbf{G}(q)) \geq 1$ everywhere. When this fails, the metric contracts relative to the Euclidean norm along the corresponding eigendirection, causing the Euclidean distance to overestimate true distances and violate admissibility.*

Algorithm 1: Loewner Meet (\mathbf{L} , \mathbf{G}_{new})

```

1  $\mathbf{S} \leftarrow \mathbf{L}^{-1} \mathbf{G}_{\text{new}} (\mathbf{L}^\top)^{-1}$ ;
2  $\mathbf{V}, \text{diag}(\lambda_1, \dots, \lambda_n) \leftarrow \text{EigenDecomposition}(\mathbf{S})$ ;
3 if  $\min_k \lambda_k < 1$  then
4    $\tilde{\lambda}_k \leftarrow \min(\lambda_k, 1)$  for each  $k \in \{1, \dots, n\}$ ;
5    $\tilde{\mathbf{\Lambda}} \leftarrow \text{diag}(\tilde{\lambda}_1, \dots, \tilde{\lambda}_n)$ ;
6    $\mathbf{G}_{\text{lower}} \leftarrow \mathbf{L} \mathbf{V} \tilde{\mathbf{\Lambda}} \mathbf{V}^\top \mathbf{L}^\top$ ;
7    $\mathbf{L} \leftarrow \text{Cholesky}(\mathbf{G}_{\text{lower}})$ ;
8 return  $\mathbf{L}$ 

```

The scalar bound (Definition 3) recovers admissibility by scaling distances uniformly; our matrix bound does so directionally, tightening only in the directions where the metric permits.

B. Computing the Loewner Lower Bound

The matrix heuristic in Definition 2 requires a constant $\mathbf{G}_{\text{lower}}$ that is dominated by $\mathbf{G}(q)$ at every configuration in \mathcal{Q} . Computing the tightest such bound is in general intractable, as it requires solving a semi-infinite program over the entire configuration space. We reduce this problem to a sequence of pairwise updates: given the current bound $\mathbf{G}_{\text{lower}}$ and a new metric evaluation \mathbf{G}_{new} , Algorithm 1 computes the *Loewner meet*, the maximal SPD matrix dominated by both.

The algorithm maintains the Cholesky factor \mathbf{L} of the current bound $\mathbf{G}_{\text{lower}}$. It first transforms \mathbf{G}_{new} into a whitened coordinate system where $\mathbf{G}_{\text{lower}}$ is the identity (Line 1). The eigenvalues of the transformed matrix \mathbf{S} indicate how \mathbf{G}_{new} compares to $\mathbf{G}_{\text{lower}}$ along each principal direction (Line 2). Eigenvalues exceeding 1 correspond to directions where \mathbf{G}_{new} already dominates $\mathbf{G}_{\text{lower}}$ and are clamped; eigenvalues less than 1 indicate directions where \mathbf{G}_{new} is smaller, requiring the bound to be loosened (Lines 4–5). Reconstructing the matrix in the original coordinate system yields the maximal lower bound of $\mathbf{G}_{\text{lower}}$ and \mathbf{G}_{new} (Line 6).

Remark 2. *Algorithm 1 is a generic subroutine: given any sequence of metric evaluations $\mathbf{G}(q_1), \dots, \mathbf{G}(q_N)$, applying it iteratively from $\mathbf{G}_{\text{lower}} = \mathbf{G}(q_1)$ yields a valid Loewner lower bound for all observed matrices. The only design choice here is the selection strategy for the configurations q_i , which can range from uniform batch sampling to targeted optimization; we detail the specific strategy used in Section VI.*

V. RIEMANNIAN INFORMED SETS

Having established an admissible distance bound in Section IV, we now show that the resulting informed set has a clean geometric characterization. By exploiting this geometry, we develop a direct, *rejection-free* sampling approach that strictly improves upon scalar-bound heuristics.

A. Isometric Embedding

The Cholesky factorization $\mathbf{G}_{\text{lower}} = \mathbf{L}\mathbf{L}^\top$ of the lower bound matrix defines a natural coordinate transformation from the configuration space \mathcal{Q} to an isotropic Euclidean space $\mathcal{X} \subseteq \mathbb{R}^n$. Under this transformation, the anisotropic weighted norm induced by $\mathbf{G}_{\text{lower}}$ reduces to the standard Euclidean norm, enabling the use of classical Euclidean geometric tools in \mathcal{X} .

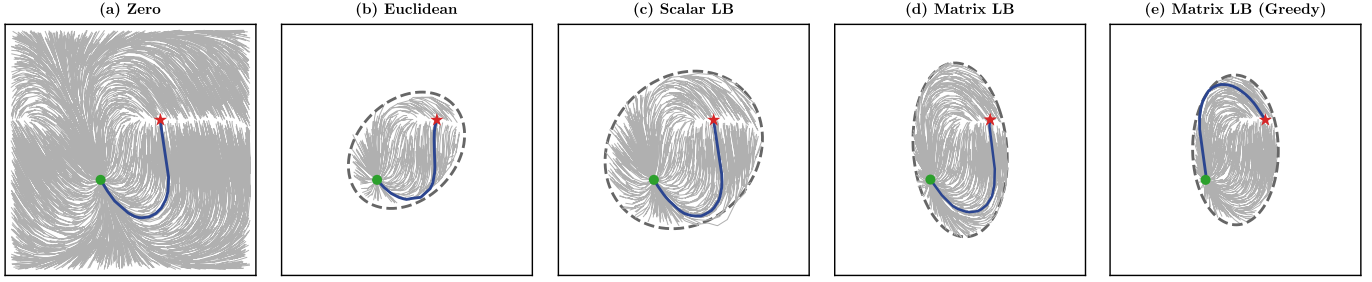


Fig. 2: Search trees and informed sets for a 2-DoF planar manipulator planning from start (●) to goal (★) under the kinetic energy Riemannian metric. (a) With no heuristic, the planner samples uniformly over \mathcal{Q} , producing a dense tree with no directional preference. (b) The Euclidean heuristic is inadmissible for this metric; the resulting isotropic prolate hyperspheroid (PHS) misguides sampling and yields a suboptimal solution. (c) The scalar eigenvalue bound produces an admissible but isotropic PHS that does not exploit the metric’s anisotropy. (d) Our matrix-valued lower bound yields an anisotropic ellipsoid aligned with the metric structure, focusing sampling along low-cost directions. (e) The greedy variant further concentrates samples near the current best solution.

Theorem 3 (Isometric embedding). *The map $\phi: \mathcal{Q} \rightarrow \mathcal{X}$ defined by $\phi(q) = \mathbf{L}^\top q$ is a linear isometry from $(\mathcal{Q}, \mathbf{G}_{\text{lower}})$ to $(\mathcal{X}, \mathbf{I})$. That is, for all $q_1, q_2 \in \mathcal{Q}$,*

$$\hat{d}(q_1, q_2) = \|\phi(q_1) - \phi(q_2)\|_2.$$

Proof. By direct computation and using Definition 4,

$$\|\phi(q_1) - \phi(q_2)\|_2 = \|\mathbf{L}^\top (q_1 - q_2)\|_2 = \hat{d}(q_1, q_2). \quad \square$$

The inverse map $\phi^{-1}(x) = \mathbf{L}^{-\top} x$ transforms points from \mathcal{X} back to the original configuration space \mathcal{Q} . We now use this isometry to characterize the geometry of the informed set. For a cost bound c_{best} , the Riemannian informed set under the matrix-valued heuristic is

$$X_f^{\mathcal{R}} = \left\{ q \in \mathcal{Q} : \hat{d}(q_{\text{start}}, q) + \hat{d}(q, q_{\text{goal}}) < c_{\text{best}} \right\}. \quad (6)$$

By Theorem 3, the heuristic sum in (6) equals $\|x_{\text{start}} - x\|_2 + \|x - x_{\text{goal}}\|_2$, where $x_{\text{start}} = \phi(q_{\text{start}})$, $x_{\text{goal}} = \phi(q_{\text{goal}})$, and $x = \phi(q)$. The set of points satisfying $\|x_{\text{start}} - x\|_2 + \|x - x_{\text{goal}}\|_2 \leq c_{\text{best}}$ is precisely a *prolate hyperspheroid* (PHS) in \mathcal{X} with foci x_{start} and x_{goal} , which we denote $X_f^{\mathcal{X}}$ [4]. Since ϕ is an invertible linear map, the preimage of $X_f^{\mathcal{X}}$ is an ellipsoid in the original configuration space.

Corollary 2 (Riemannian informed set is an ellipsoid). *The Riemannian informed set $X_f^{\mathcal{R}}$ in (6) satisfies*

$$X_f^{\mathcal{R}} = \phi^{-1}(X_f^{\mathcal{X}}). \quad (7)$$

In the original coordinates, $X_f^{\mathcal{R}}$ under $\mathbf{G}_{\text{lower}} = \mathbf{L}\mathbf{L}^\top$ is an ellipsoid whose principal axes are rotated and scaled by $\mathbf{L}^{-\top}$ relative to those of $X_f^{\mathcal{X}}$.

Compared to the scalar bound (Definition 3), which produces an isotropic PHS regardless of the metric’s anisotropy, the matrix bound produces an ellipsoid that is elongated along low-cost directions and compressed along high-cost directions. Consequently, this directional structure of $X_f^{\mathcal{R}}$ focuses sampling in regions most likely to improve the current solution.

B. Direct Sampling

The ellipsoidal characterization in Corollary 2 enables a direct sampling procedure for $X_f^{\mathcal{R}}$. Instead of drawing samples from the entire \mathcal{Q} and rejecting those outside $X_f^{\mathcal{R}}$, we sample uniformly from $X_f^{\mathcal{X}}$ in the isotropic space and transform back

Algorithm 2: Sampling from $X_f^{\mathcal{R}}$ ($\mathbf{L}, q_{\text{start}}, q_{\text{goal}}, c_{\text{best}}$)

- 1 $x_{\text{start}} \leftarrow \mathbf{L}^\top q_{\text{start}}, x_{\text{goal}} \leftarrow \mathbf{L}^\top q_{\text{goal}};$
 - 2 $x \leftarrow \text{Uniform}(X_f^{\mathcal{X}});$
 - 3 $q \leftarrow \mathbf{L}^{-\top} x;$
 - 4 **if** $q \in \mathcal{Q}$ **then**
 - 5 **return** $q;$
 - 6 **return** reject and resample
-

to \mathcal{Q} . This procedure, presented in Algorithm 2, produces uniform samples on $X_f^{\mathcal{R}}$ without any geometric rejection.

The algorithm first maps q_{start} and q_{goal} to \mathcal{X} via ϕ (Line 1). It then draws a uniform sample from $X_f^{\mathcal{X}}$ using the standard PHS decomposition of [4] (Line 2). Finally, it maps the sample back to the original configuration space \mathcal{Q} via ϕ^{-1} (Line 3). Because ϕ^{-1} is an invertible linear map, the change of variables preserves uniformity with respect to the Lebesgue measure: the resulting sample is uniform on $X_f^{\mathcal{R}} \subset \mathcal{Q}$ in the same sense as in standard Euclidean informed sampling [4]³. The only source of rejection is bound satisfaction, that is, the ellipsoid may extend beyond \mathcal{Q} (Line 4), which is identical to the rejection that arises in standard Euclidean PHS sampling [4]. There is no additional geometric rejection from the informed set itself, unlike heuristic-guided rejection sampling for generic distance functions.

C. Geometric Interpretation

The spectral decomposition of $\mathbf{G}_{\text{lower}}$ provides a concrete geometric picture of the Riemannian informed set. Let $\mathbf{G}_{\text{lower}} = \mathbf{V}\mathbf{\Lambda}\mathbf{V}^\top$ be the eigendecomposition, where each column of \mathbf{V} is an eigenvector with associated eigenvalue λ_i . Each eigenvector defines a principal direction of the metric lower bound, and the corresponding eigenvalue encodes the cost of motion along that direction. The isometry $\phi(q) = \mathbf{L}^\top q$ rotates the configuration space to align with these principal directions and scales each axis by $\sqrt{\lambda_i}$, so that all directions carry equal cost in \mathcal{X} . The inverse map ϕ^{-1} reverses this normalization, warping the isotropic PHS $X_f^{\mathcal{X}}$ into the anisotropic ellipsoid $X_f^{\mathcal{R}}$ in the original coordinates. Each principal axis of $X_f^{\mathcal{R}}$ is scaled by $1/\sqrt{\lambda_i(\mathbf{G}_{\text{lower}})}$ relative to those of the PHS, that is, the ellipsoid extends further along directions where motion is inexpensive and contracts where it is costly.

³This is uniformity with respect to the Lebesgue measure on \mathcal{Q} , not the true Riemannian volume induced by $\mathbf{G}(q)$; the latter would require knowledge of the full metric field, which our heuristic explicitly avoids.

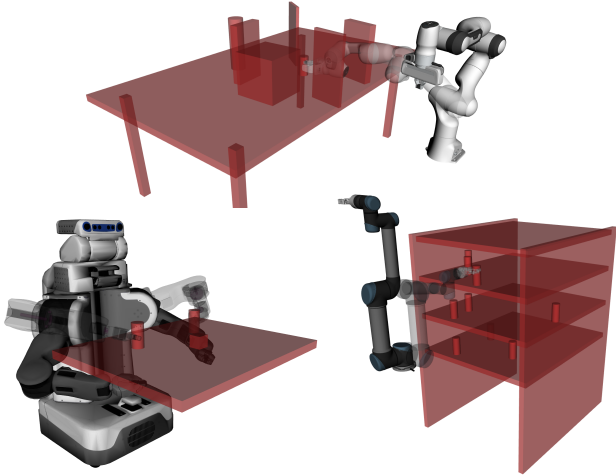


Fig. 3: Planning scenes for the manipulation experiments in Section VI-B.

This ellipsoidal characterization also yields a closed-form expression for the Lebesgue measure (volume) of the Riemannian informed set $X_f^{\mathcal{R}}$; note that this upper bounds the volume of the true Riemannian informed set defined by the geodesic distance d , i.e., $\mathcal{X}_f^{\mathcal{R}} \subseteq X_f^{\mathcal{R}}$. Let $\mu(\cdot)$ denote the Lebesgue measure in \mathbb{R}^n . Since ϕ^{-1} is a linear map with Jacobian determinant $1/\sqrt{\det(\mathbf{G}_{\text{lower}})}$, the change-of-variables formula gives

$$\mu(X_f^{\mathcal{R}}) = \frac{\mu_{\text{PHS}}(c_{\text{best}}, d_{\text{foci}})}{\sqrt{\det(\mathbf{G}_{\text{lower}})}}, \quad (8)$$

where $d_{\text{foci}} = \hat{d}(q_{\text{start}}, q_{\text{goal}})$ is the heuristic distance between start and goal, and $\mu_{\text{PHS}}(c, d)$ denotes the known Lebesgue measure of an n -dimensional PHS with transverse diameter c and focal distance d [4].

Equation (8) shows that the matrix bound reduces the informed set’s volume through two independent mechanisms. First, because $\hat{d} \geq \hat{d}_\lambda$, d_{foci} is larger under the matrix bound, producing a thinner PHS in the isotropic space and reducing the numerator. Second, the denominator $\sqrt{\det(\mathbf{G}_{\text{lower}})} = \sqrt{\prod_{i=1}^n \lambda_i(\mathbf{G}_{\text{lower}})}$ grows with the full eigenspectrum of $\mathbf{G}_{\text{lower}}$, not just its minimum eigenvalue as under the scalar bound, yielding a strictly smaller informed set whenever $\mathbf{G}_{\text{lower}}$ is anisotropic. In high dimensions, even modest per-direction improvements accumulate multiplicatively through the determinant, producing informed sets that are orders of magnitude smaller than their scalar counterparts.

VI. EXPERIMENTS

We evaluate our matrix-valued heuristic on manipulation problems from the MotionBenchMaker dataset [40], spanning three robots of increasing dimensionality: a 6-DoF UR5, a 7-DoF Franka, and a 14-DoF PR2 dual-arm system (Figure 3). For each robot, we consider three Riemannian metrics: a diagonal weighted metric, the kinetic energy metric derived from the robot’s mass matrix, and a pullback metric induced by the manipulator Jacobian. The weighted metric penalizes unnecessary joint motion by assigning a weight of 100 to joints with small start-to-goal displacement and 1 otherwise. The pullback metric uses a regularization value of 0.1 to ensure positive-definiteness near singularities. All experiments

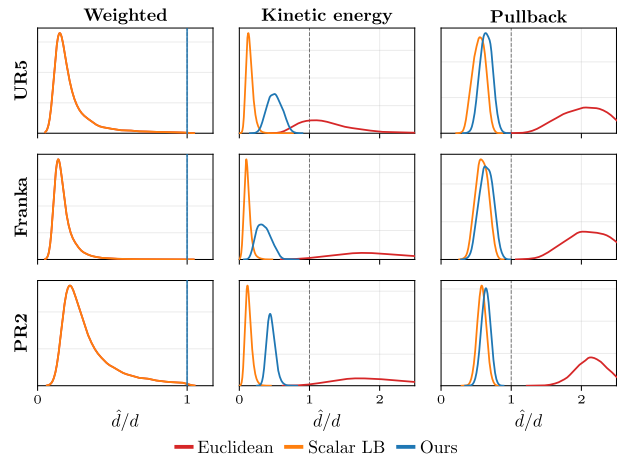


Fig. 4: Distribution of the heuristic-to-geodesic-distance ratio \hat{d}/d for 10,000 random configuration pairs across all three robots and metrics; the dashed line marks the admissibility threshold at ratio 1.

minimize the Riemannian arc length (1) under the given metric, using the midpoint approximation of [8].

We compare five asymptotically optimal sampling-based planners, BIT* [3], AIT* and EIT* [13], GRRT* [14], and AORRTC [41], each evaluated under three heuristic configurations: the Euclidean distance, the zero heuristic ($\hat{d} = 0$), and our proposed Loewner lower bound. For GRRT*, we set the greedy biasing ratio to $\epsilon = 0$, which disables greedy exploitation and reduces the planner to an informed variant of RRT*-Connect [42]. We also include GRRT* with $\epsilon = 0.9$ and matrix-valued heuristic to demonstrate that greedy informed sampling further accelerates convergence when combined with the Loewner bound. The scalar eigenvalue bound is omitted from the main comparison; the ablation in Section VI-A confirms that it is consistently looser than the matrix bound across all robots and metrics, making it redundant as a separate baseline.

All planners are implemented in C++ using the Open Motion Planning Library (OMPL) [43] with VAMP’s collision checking backend [44]. The kinetic energy metric uses the mass matrix computed via Pinocchio library [45]. The Loewner lower bound $\mathbf{G}_{\text{lower}}$ is precomputed for each robot–metric pair via Algorithm 1, using an optimization-based approach to select metric evaluation points rather than uniform random sampling (Appendix I). We find that this approach converges to a tighter bound more efficiently, particularly in high dimensions. For each scenario, we run 100 trials with different pseudorandom seeds and a planning budget of 120 s, and report the median solution cost as a function of planning time.

A. Heuristic Quality

This section evaluates the tightness of each heuristic to validate Theorem 2 empirically. For each robot and metric, we sample 10,000 random configuration pairs and compute the ratio $\hat{d}(\cdot)/d(\cdot)$, where d is the numerically estimated geodesic distance. A ratio of 1 indicates a perfect heuristic; below 1 is admissible; above 1 is inadmissible.

Figure 4 shows the heuristic ratio distributions across all robots and metrics. The Euclidean heuristic is inadmissible under the kinetic energy and pullback metrics, with median ratios exceeding 1 in all scenarios, confirming that it is unsuitable as a cost-to-go estimate on non-Euclidean spaces.

Algorithm 3: Loewner lower bound (q_{init}, τ)

```
1  $\mathbf{L} \leftarrow \text{Cholesky}(\mathbf{G}(q_{\text{init}}));$ 
2 repeat
3    $q^* \leftarrow \text{argmin}_q \lambda_{\min}(\mathbf{L}^{-1} \mathbf{G}(q) \mathbf{L}^{-\top});$ 
4    $\lambda^* \leftarrow \lambda_{\min}(\mathbf{L}^{-1} \mathbf{G}(q^*) \mathbf{L}^{-\top});$ 
5   if  $\lambda^* < 1 - \tau$  then
6      $\mathbf{L} \leftarrow \text{LoewnerMeet}(\mathbf{L}, \mathbf{G}(q^*));$  // Alg. 1
7 until  $\lambda^* \geq 1 - \tau;$ 
8 return  $\mathbf{G}_{\text{lower}} = \mathbf{L}\mathbf{L}^\top$ 
```

The scalar bound is always admissible but highly conservative. Under the constant weighted metric, the matrix bound recovers the geodesic distance exactly (a ratio of 1), trivially validating the approach since $\mathbf{G}_{\text{lower}} = \mathbf{G}$. The advantage is most pronounced under the kinetic energy metric, where the matrix bound is 3–4 times tighter than the scalar bound, capturing the directional structure of the inertia tensor. Under the pullback metric, λ -regularization near kinematic singularities makes $\mathbf{G}_{\text{lower}}$ nearly isotropic, limiting improvement over the scalar bound to approximately 10–15%. These per-metric differences directly explain the convergence patterns in Section VI-B.

B. Manipulation Problems

Figure 5 shows median solution cost versus planning time across all nine robot–metric scenarios. Under the weighted and kinetic energy metrics, planners with the matrix bound consistently converge faster than zero-heuristic and Euclidean counterparts, with the degree of improvement varying across planners and robot dimensionality. The improvement is most pronounced under the kinetic energy metric, consistent with the 3–4 times tighter heuristic ratios reported in Section VI-A.

Under the pullback metric, the inadmissible Euclidean heuristic traps planners in local minima on the UR5 and Franka tasks, failing to converge within the time budget. The PR2 is an exception: despite large overestimation, the Euclidean heuristic converges well, as the overestimate coincidentally guides search toward better solutions on this problem instance. Conversely, the matrix bound offers only modest improvement, as regularization term near singularities makes $\mathbf{G}_{\text{lower}}$ nearly isotropic, collapsing its directional advantage as predicted in Section VI-A.

The fastest convergence is achieved with GRRT* ($\epsilon = 0.9$) under the matrix bound, across all robots and metrics. Even when the bound becomes nearly isotropic and the informed set offers limited benefit, direct sampling in the isotropic Euclidean space still enables GRRT* to exploit its greedy biasing, maintaining its advantage over all baselines. AORRTC with the matrix bound also converges faster than its other variants, though the zero-heuristic variant remains competitive across all metrics; heuristic quality affects only the informed sampling step in AORRTC’s cost-augmented search.

VII. CONCLUSION

This work presented a *matrix-valued* admissible heuristic for informed sampling in motion planning under configuration-dependent Riemannian metrics. The key insight is that a constant Loewner lower bound on the metric tensor preserves directional structure, yielding tighter informed sets than the

scalar eigenvalue bound while remaining provably admissible. Its Cholesky factorization reduces the Riemannian informed set to a standard prolate hyperspheroid in isotropic Euclidean space, enabling direct sampling with existing techniques. Across nine manipulation scenarios spanning three robots and three metrics, our heuristic consistently accelerates convergence across multiple asymptotically optimal planners, with the largest gains under anisotropic metrics where directional structure is most informative. Future work will investigate tighter bounds for heavily regularized metrics, where the current approach degenerates toward the scalar bound. We are also interested in extending the framework to non-Euclidean cost functions where an explicit metric tensor is unavailable.

APPENDIX I OPTIMIZATION-BASED BOUND COMPUTATION

We initialize $\mathbf{G}_{\text{lower}}$ with the metric evaluated at q_{init} , set to the midpoint of the joint limits, and iteratively search for q^* via multi-start gradient descent with Armijo backtracking (Algorithm 3). At each iteration, q^* is the configuration with the largest deviation between $\mathbf{G}(q)$ and the current bound; we then tighten $\mathbf{G}_{\text{lower}}$ via Algorithm 1. The process terminates when $\lambda^* \geq 1 - \tau$ for all found optima, which certifies $\mathbf{G}_{\text{lower}} \preceq \mathbf{G}(q)$ over the explored space. We use $\tau = 10^{-6}$ in all experiments.

REFERENCES

- [1] S. M. LaValle and J. J. Kuffner Jr, “Randomized kinodynamic planning,” *Int. J. Robot. Res.*, vol. 20, no. 5, pp. 378–400, 2001.
- [2] S. Karaman and E. Frazzoli, “Sampling-based algorithms for optimal motion planning,” *Int. J. Robot. Res.*, vol. 30, no. 7, pp. 846–894, 2011.
- [3] J. D. Gammell, T. D. Barfoot, and S. S. Srinivasa, “Batch Informed Trees (BIT*): Informed asymptotically optimal anytime search,” *Int. J. Robot. Res.*, vol. 39, no. 5, pp. 543–567, 2020.
- [4] —, “Informed sampling for asymptotically optimal path planning,” *IEEE Trans. Robot.*, vol. 34, no. 4, pp. 966–984, 2018.
- [5] F. Bullo and A. D. Lewis, *Geometric control of mechanical systems: modeling, analysis, and design for simple mechanical control systems*. Springer, 2019, vol. 49.
- [6] N. Jaquier and T. Asfour, “Riemannian geometry as a unifying theory for robot motion learning and control,” in *Proc. Int. Symp. Robot. Res. (ISR)*. Springer, 2022, pp. 395–403.
- [7] Y. Li, J. Qiu, and S. Calinon, “A Riemannian take on distance fields and geodesic flows in robotics,” *Int. J. Robot. Res.*, p. 02783649261420233, 2024.
- [8] P. T. Kyaw and J. Kelly, “Geometry-aware sampling-based motion planning on Riemannian manifolds,” *arXiv preprint arXiv:2602.00992*, 2026.
- [9] N. Jaquier, L. Roza, D. G. Caldwell, and S. Calinon, “Geometry-aware manipulability learning, tracking, and transfer,” *Int. J. Robot. Res.*, vol. 40, no. 2-3, pp. 624–650, 2021.
- [10] M. Saveriano, F. J. Abu-Dakka, and V. Kyrki, “Learning stable robotic skills on Riemannian manifolds,” *Robot. Auton. Syst.*, vol. 169, p. 104510, 2023.
- [11] F. Marić, L. Petrović, M. Guberina, J. Kelly, and I. Petrović, “A Riemannian metric for geometry-aware singularity avoidance by articulated robots,” *Robot. Auton. Syst.*, vol. 145, p. 103865, 2021.
- [12] G. Peyré and L. D. Cohen, “Geodesic methods for shape and surface processing,” *Adv. Comput. Vis. Med. Image Process.*, pp. 29–56, 2009.
- [13] M. P. Strub and J. D. Gammell, “Adaptively Informed Trees (AIT*) and Effort Informed Trees (EIT*): Asymmetric bidirectional sampling-based path planning,” *Int. J. Robot. Res.*, vol. 41, no. 4, pp. 390–417, 2022.
- [14] P. T. Kyaw, A. V. Le, R. E. Mohan, and J. Kelly, “Greedy heuristics for sampling-based motion planning in high-dimensional state spaces,” *arXiv preprint arXiv:2405.03411*, 2024.
- [15] J. Sehn, T. D. Barfoot, and J. Collier, “Off the beaten track: Laterally weighted motion planning for local obstacle avoidance,” *IEEE Trans. Field Robot.*, vol. 1, pp. 249–275, 2024.

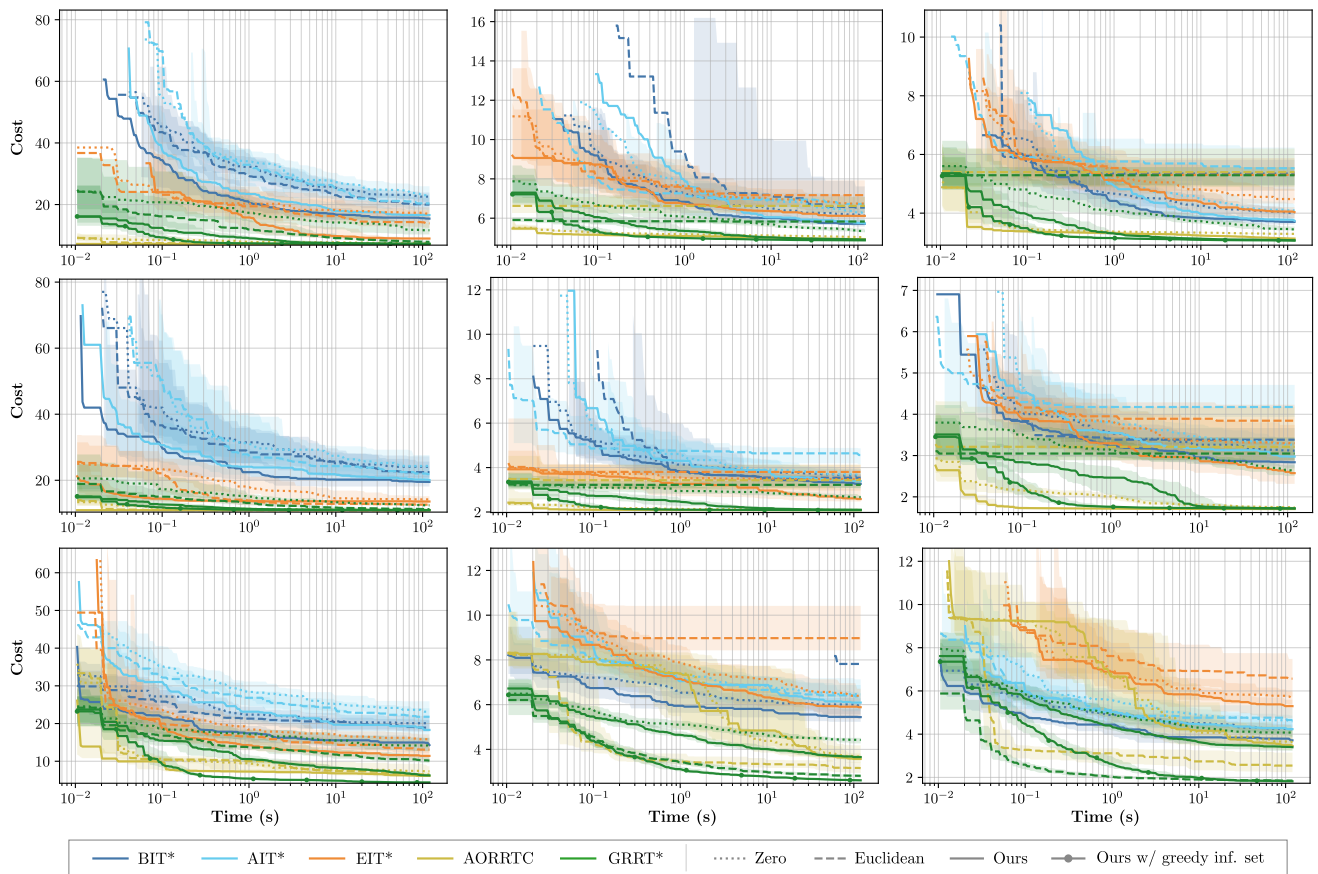


Fig. 5: Anytime planning performance across all nine robot–metric scenarios over 100 trials. Rows correspond to robots (top to bottom: UR5, Franka, PR2) and columns to metrics (left to right: weighted Euclidean, kinetic energy, pullback). Each panel plots median solution cost against planning time for all tested planners under the zero, Euclidean, and matrix lower bound heuristics; shaded regions denote non-parametric 99% confidence intervals on the median.

- [16] D. Yi, R. Thakker, C. Gulino, O. Salzman, and S. Srinivasa, “Generalizing informed sampling for asymptotically-optimal sampling-based kinodynamic planning via markov chain monte carlo,” in *Proc. IEEE Int. Conf. Robot. Autom. (ICRA)*, 2018, pp. 7063–7070.
- [17] T. Kunz, A. Thomaz, and H. Christensen, “Hierarchical rejection sampling for informed kinodynamic planning in high-dimensional spaces,” in *Proc. IEEE Int. Conf. Robot. Autom. (ICRA)*, 2016, pp. 89–96.
- [18] J. D. Gammell and M. P. Strub, “Asymptotically optimal sampling-based motion planning methods,” *Annu. Rev. Control Robot. Auton. Syst.*, vol. 4, no. 1, pp. 295–318, 2021.
- [19] B. Paden, V. Varricchio, and E. Frazzoli, “Verification and synthesis of admissible heuristics for kinodynamic motion planning,” *IEEE Robot. Autom. Lett.*, vol. 2, no. 2, pp. 648–655, 2017.
- [20] M. Przybylski, “Asymptotically optimal A* for kinodynamic planning,” *IEEE Robot. Autom. Lett.*, vol. 9, no. 5, pp. 4353–4360, 2024.
- [21] B. Sakcak, L. Bascetta, G. Ferretti, and M. Prandini, “An admissible heuristic to improve convergence in kinodynamic planners using motion primitives,” *IEEE Control Syst. Lett.*, vol. 4, no. 1, pp. 175–180, 2019.
- [22] S. Liu, K. Mohta, N. Atanasov, and V. Kumar, “Search-based motion planning for aggressive flight in SE(3),” *IEEE Robot. Autom. Lett.*, vol. 3, no. 3, pp. 2439–2446, 2018.
- [23] V. Surazhsky, T. Surazhsky, D. Kirsanov, S. J. Gortler, and H. Hoppe, “Fast exact and approximate geodesics on meshes,” *ACM Trans. Graph.*, vol. 24, no. 3, pp. 553–560, 2005.
- [24] G. Peyre and L. D. Cohen, “Landmark-based geodesic computation for heuristically driven path planning,” in *Proc. IEEE Conf. Comput. Vis. Pattern Recognit. (CVPR)*, vol. 2, 2006, pp. 2229–2236.
- [25] B. Paden, Y. Nager, and E. Frazzoli, “Landmark guided probabilistic roadmap queries,” in *Proc. IEEE/RSJ Int. Conf. Intell. Robots Syst. (IROS)*, 2017, pp. 4828–4834.
- [26] J.-M. Mirebeau, “Riemannian fast-marching on cartesian grids, using Voronoi’s first reduction of quadratic forms,” *SIAM J. Numer. Anal.*, vol. 57, no. 6, pp. 2608–2655, 2019.
- [27] T. Cohn, M. Petersen, M. Simchowitz, and R. Tedrake, “Non-Euclidean motion planning with graphs of geodesically convex sets,” *Int. J. Robot. Res.*, vol. 44, no. 10-11, pp. 1840–1862, 2025.
- [28] A. Lukyanenko and D. Soudbakhsh, “Probabilistic motion planning for non-Euclidean and multi-vehicle problems,” *Robot. Auton. Syst.*, vol. 168, p. 104487, 2023.
- [29] S. Boyd, L. El Ghaoui, E. Feron, and V. Balakrishnan, *Linear matrix inequalities in system and control theory*. SIAM, 1994.
- [30] S. D. Bopardikar, B. Englot, A. Speranzon, and J. van den Berg, “Robust belief space planning under intermittent sensing via a maximum eigenvalue-based bound,” *Int. J. Robot. Res.*, vol. 35, no. 13, pp. 1609–1626, 2016.
- [31] T. Shan and B. Englot, “Belief roadmap search: Advances in optimal and efficient planning under uncertainty,” in *Proc. IEEE/RSJ Int. Conf. Intell. Robots Syst. (IROS)*, 2017, pp. 5318–5325.
- [32] S. Singh, A. Majumdar, J.-J. Slotine, and M. Pavone, “Robust online motion planning via contraction theory and convex optimization,” in *Proc. IEEE Int. Conf. Robot. Autom. (ICRA)*, 2017, pp. 5883–5890.
- [33] M. Kalakrishnan, S. Chitta, E. Theodorou, P. Pastor, and S. Schaal, “STOMP: Stochastic trajectory optimization for motion planning,” in *Proc. IEEE Int. Conf. Robot. Autom. (ICRA)*, 2011, pp. 4569–4574.
- [34] M. Zucker, N. Ratliff, A. D. Dragan, M. Pivtoraiko, M. Klingensmith, C. M. Dellin, J. A. Bagnell, and S. S. Srinivasa, “CHOMP: Covariant hamiltonian optimization for motion planning,” *Int. J. Robot. Res.*, vol. 32, no. 9-10, pp. 1164–1193, 2013.
- [35] R. Deits and R. Tedrake, “Computing large convex regions of obstacle-free space through semidefinite programming,” in *Proc. Workshop Algorithmic Found. Robot. (WAFR)*. Springer, 2015, pp. 109–124.
- [36] C. Holmes, F. Dümbgen, and T. Barfoot, “On semidefinite relaxations for matrix-weighted state-estimation problems in robotics,” *IEEE Trans. Robot.*, vol. 40, pp. 4805–4824, 2024.
- [37] J. M. Lee, *Introduction to Riemannian Manifolds*. Springer, 2018, vol. 2.
- [38] R. Bhatia, *Positive Definite Matrices*. Princeton University Press, 2007.
- [39] R. V. Kadison, “Order properties of bounded self-adjoint operators,” *Proc. Amer. Math. Soc.*, vol. 2, no. 3, pp. 505–510, 1951.
- [40] C. Chamzas, C. Quintero-Pena, Z. Kingston, A. Orthey, D. Rakita,

- M. Gleicher, M. Toussaint, and L. E. Kavraki, "MotionBenchMaker: A tool to generate and benchmark motion planning datasets," *IEEE Robot. Autom. Lett.*, vol. 7, no. 2, pp. 882–889, 2022.
- [41] T. S. Wilson, W. Thomason, Z. Kingston, and J. D. Gammell, "AORRTC: Almost-surely asymptotically optimal planning with RRT-Connect," *IEEE Robot. Autom. Lett.*, 2025.
- [42] S. Klemm, J. Oberländer, A. Hermann, A. Roennau, T. Schamm, J. M. Zollner, and R. Dillmann, "RRT*-Connect: Faster, asymptotically optimal motion planning," in *Proc. IEEE Int. Conf. Robot. Biomimetics (ROBIO)*, 2015, pp. 1670–1677.
- [43] I. A. Sucas, M. Moll, and L. E. Kavraki, "The open motion planning library," *IEEE Robot. Autom. Mag.*, vol. 19, no. 4, pp. 72–82, 2012.
- [44] W. Thomason, Z. Kingston, and L. E. Kavraki, "Motions in microseconds via vectorized sampling-based planning," in *Proc. IEEE Int. Conf. Robot. Autom. (ICRA)*, 2024, pp. 8749–8756.
- [45] J. Carpentier, G. Saurel, G. Buondonno, J. Mirabel, F. Lamiroux, O. Stasse, and N. Mansard, "The Pinocchio C++ library: A fast and flexible implementation of rigid body dynamics algorithms and their analytical derivatives," in *Proc. IEEE/SICE Int. Symp. Syst. Integr. (SII)*, 2019, pp. 614–619.